JCTC Journal of Chemical Theory and Computation

Local Bonding Effects in the Oxidation of CO on Oxygen-Covered Au(111) from Ab Initio Molecular Dynamics Simulations

Thomas A. Baker,[†] Cynthia M. Friend,*[,†,‡] and Efthimios Kaxiras[†,‡,§]

Department of Chemistry and Chemical Biology, Harvard University, 12 Oxford St, Cambridge, Massachusetts 02138, School of Engineering and Applied Sciences, Harvard University, Cambridge, Massachusetts 02138, and Department of Physics, Harvard University, 16 Oxford St., Cambridge, Massachusetts 02139

Received August 28, 2009

Abstract: A fully dynamical approach using ab initio molecular dynamics (AIMD) simulations is applied to the investigation of CO oxidation on O-covered Au(111). We investigate how the activity of gold depends upon temperature, oxygen coverage, and surface structure. On clean Au(111) at 500 K, CO binds transiently on top of Au atoms, spending a small fraction (∼7%) of the total simulation time adsorbed on the surface. The presence of O on the surface increases the residence time for CO by more than 4 times on a surface containing 0.22 ML of O. On the other hand, the probability for CO adsorption decreases with oxygen coverage from 31% at 0.22 ML of oxygen to 15% at 0.55 ML of oxygen. Our simulations show that the activity for CO reaction with O to yield CO_2 decreases with increasing oxygen coverage. We attribute this decrease of activity to (1) the decrease in the CO adsorption probability as the oxygen coverage increases and (2) the decreasing amount of reactive chemisorbed oxygen (oxygen bound in a 3-fold site) with increasing total oxygen coverage. We show that oxygen bound in sites of local 3-fold coordination (chemisorbed oxygen) is nearly 2 times more reactive than other oxygen species observed on the surface, namely, surface and subsurface oxide. Our work demonstrates the value and feasibility of using AIMD to study surface reactions.

I. Introduction

Since the discovery[1–8] that gold nanoparticles supported on reducible metal oxides are catalytically active for many processes, including CO oxidation,[9] there is renewed interest in the potential use of gold as a material for low-temperature selective oxidation catalysis. The detailed understanding of the interaction of adsorbed oxygen and CO with the Au(111) surface is important because oxidized Au(111) is a model system for understanding chemical processes relevant to heterogeneous catalysis. While the oxidation of CO on gold has been studied extensively both experimentally[10–20] and theoretically,[21–39] there are still unanswered questions regarding the activity of gold. One specific issue is how the local bonding of oxygen affects the activity for CO oxidation. It is, therefore, critical to determine the oxygen species and structure that prevail under different conditions.

Previous experimental studies[16] showed that ozone efficiently dissociates to form atomic oxygen on Au(111) and that the local bonding and surface morphology depend on the surface temperature during exposure to O_3. In turn, the state of the surface has a significant effect on the activity for CO oxidation. Scanning tunneling microscopy (STM) studies revealed differences in the surface morphology depending on the temperature used for oxidation or the coverage of atomic oxygen.[11] High-resolution electron energy loss and X-ray photoelectron spectroscopies also showed that the local bonding of oxygen depends on the oxidation temperature and the oxygen coverage. Detailed studies of

* Corresponding author. Tel: 617-495-4052. Fax: 617-496-8410. E-mail: friend@chemistry.harvard.edu.

[†] Department of Chemistry and Chemical Biology.

[‡] School of Engineering and Applied Sciences.

[§] Department of Physics.

10.1021/ct9004596
Published on Web 12/03/2009

the activity for CO oxidation on O-covered Au(111) suggested that the activity for CO oxidation varies significantly for different types of oxygen (chemisorbed versus a surface oxide).

In addition to local bonding of O, the structure of the Au is thought to play a role in determining reactivity. Liu et al.,[26] using density functional theory (DFT) calculations, reported that the energy barrier for CO oxidation depends on the crystal face of the stepped surface. Recently, we also found differences in the calculated energy barrier, depending on the type of surface defect used, for the reaction of propene with atomic oxygen on Au(111).[40] Structure also plays a vital role for oxide-supported Au nanoparticles, since the size[41,42] and the particle shape[43] have a substantial effect on the reactivity, with rate constants differing by as much as 2 orders of magnitude.[32] It is clear that the oxygen surface species and surface morphology, which are strongly correlated for the Au−O interaction, play an important role in the reactivity of the gold surface.

While experimental studies clearly show that atomic O bound to Au is highly active for CO oxidation, there is still controversy about the types of oxygen that react with the CO. Clearly, atomic O is very active for CO oxidation; however, O_2 dissociation is required. A second reaction scenario involves molecular O_2 adsorption followed by CO adsorption and reaction to make a peroxo-like, $OC\cdots O_2$ complex, which leads to CO_2 and residual atomic oxygen. Criticism of the first mechanism is based on the fact that the dissociation rate of O_2 on gold surfaces is low, consistent with DFT calculations that find a high energy barrier for O_2 dissociation even on small clusters,[26,44–46] and on recent work showing the role of molecular O_2 in oxidation.[13,47] In contrast to other transition-metal surfaces, there is no appreciable O_2 dissociation on extended single crystals of Au.[48] As a result, experimental studies use other sources of oxygen to produce atomic oxygen on the surface.[49–53] Nevertheless, atomic oxygen is ultimately formed even in the scenario where O_2 reacts directly with CO; thus, it is important to understand the reactivity of O on gold.

Temperature is an important factor in determining the morphology and ultimately the reactivity of the surface. Treatment of surface temperature is a major challenge for theoretical studies, and for this reason, previous theoretical investigations of CO oxidation on Au surfaces have generally used static, zero-temperature DFT calculations. Kinetic Monte Carlo (kMC) is a popular theoretical technique for modeling the dynamical temperature dependence on the reactivity of a surface[54] and has been effectively used to model CO oxidation on $RuO_2(110)$.[55] Unfortunately, kMC methods presume prior knowledge of all the events important to the dynamics of the system. Furthermore, the spatial degrees of freedom of the system are typically reduced to a simple lattice. The interaction of oxygen with Au is complex because of the role of defects and metal atom release. Therefore, it is impossible to know all the important events a priori and it is unrealistic to confine these events within the context of a lattice. Ideally, one wants to capture all the relevant effects in a fully atomistic molecular dynamics simulation with accurate forces between ions and under realistic external conditions (temperature and oxygen concentration).

Molecular dynamics is an important tool for simulating reactions and other dynamical chemical behavior for a variety of systems, including surfaces.[56] Classical force fields, which can be derived from many sources including first-principle methods or empirical observations, are used to describe the interaction of atoms and have been used in many applications. These force fields can be useful because they are computationally cheap, giving the ability to simulate large systems for long time scales (easily thousands of atoms for nanoseconds). The disadvantage of these force fields is their poor accuracy—classical or course-grained methods often do not capture complex chemical behavior, including bond breaking and formation. Ab initio molecular dynamics (AIMD), that is, using first-principles for calculating forces, provides a more accurate alternative to classical methods and has been used in many situations to understand surfaces.[57,58] Typically, AIMD calculations employ the Born−Oppenheimer approximation, but it is important to point out that for catalytic reactions on surfaces there are some cases where there is electronic nonadiabatic coupling, making the Born−Oppenheimer approximation invalid.[59,60] Other important molecular dynamics methods that could be useful for understanding the dynamics of surfaces include (but are not limited to) Car−Parrinello dynamics[61] or Ehrenfest dynamics.[62,63] The challenge in performing AIMD simulations is the restriction to short time scales because the calculations are computationally expensive.

Recently, we have developed the ability to use AIMD simulations to model the *dynamic* restructuring of the Au(111) surface due to the adsorption of atomic oxygen and have obtained results that are in agreement with vibrational spectroscopy experiments.[64] We find that the morphology and fraction of various O bonding configurations depend on the coverage and temperature at the tested coverages of 0.22, 0.33, and 0.55 monolayers (ML), and at 200, 500, and 800 K.[64] We categorized oxygen into three different types: chemisorbed oxygen, surface oxide, and subsurface oxide, as illustrated in Figure 1. These three types represent, respectively, an oxygen atom bound on top of the surface in a 3-fold hollow site, an oxygen atom bound to a gold atom that has been pulled out of the surface, and an oxygen atom buried below the first layer of gold. At low oxygen coverage (<0.33 ML) or temperature (200 K), the Au(111) surface is smooth and contains mostly chemisorbed oxygen, while at higher coverage (>0.33 ML) or temperature (500, 800 K), it is oxidized, containing a higher concentration of surface and subsurface oxide. By matching calculated vibrational spectra with the experimental results under conditions that produce the most reactive surface for CO and olefin oxidation (low coverage and low temperature), we suggested that chemisorbed oxygen was the more reactive type of oxygen for CO oxidation on Au(111).

Herein, we report a detailed study of CO oxidation on O-covered Au(111) using AIMD. We directly confirm that chemisorbed oxygen, i.e., O bound to sites of local 3-fold coordination, is most reactive. We also discuss the underlying

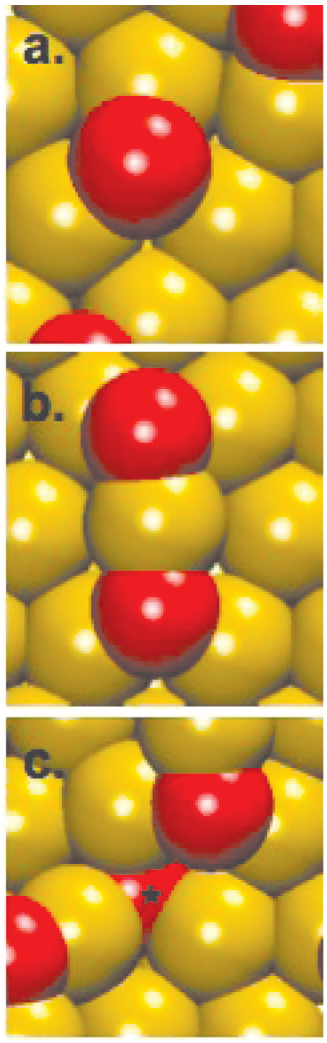

Figure 1. Model (top view) of three oxygen types: (a) chemisorbed, (b) surface oxide, and (c) subsurface oxide (labeled by an asterisk). Yellow and red spheres represent gold and oxygen atoms, respectively.

physical reasons for this different reactivity and place it in a broader context of using AIMD to model the dynamics of surface reactions.

II. Calculational Details

We performed the AIMD simulations in the canonical ensemble,[65] with a time step of 2 fs, for the reaction of carbon monoxide with atomic oxygen covered Au(111) in the framework of density functional theory using the VASP code[66] with the GGA-PW91[67] functional and ultrasoft pseudopotentials.[68,69] We used a plane-wave cutoff energy of 300.0 eV, an electronic convergence tolerance of 10^{-3} eV, and $2 \times 2 \times 1$ Monkhorst−Pack reciprocal space (*k*-point) sampling. The surface is modeled by a slab consisting of four layers in the (111) direction, with a 3×3 supercell in the lateral directions; the three uppermost layers of the slab were allowed to relax, with the bottom layer fixed at the ideal bulk positions.

We considered four different conditions: clean Au(111) and Au(111) with O coverages of 0.22, 0.33, and 0.55 ML at 500 K. The simulation temperature of 500 K represents an optimal balance of adsorption and reaction, thus minimizing the total simulation time needed to observe important events in the system. The surfaces were prepared as follows:[64] oxygen was randomly placed above an equilibrated Au(111) substrate and the system then simulated at 500 K for 2 ps to allow for adsorption and rearrangement of the surface. To model the reaction of CO with these substrates, one CO molecule (0.11 ML coverage) was introduced to each system with a zero initial velocity, ∼3 Å above the surface. For this reason, we are unable to find a sticking probability to compare with experiment, defined as the ratio of the adsorption rate to impingement rate,[70] since for a molecular beam or a background gas there would be molecules hitting the surface with either a nonzero constant velocity or Maxwell−Boltzmann distribution of velocities. In contrast, our simulations are limited to CO molecules with a zero initial velocity above the surface so as to increase the probability of adsorption, thus significantly overestimating the true sticking probability.

At each oxygen coverage, 100 independent simulations were performed, each lasting 8 ps. All results are obtained after a sufficient equilibration time, as evaluated by the point in time at which fluctuations in the average energy, temperature, and other measurable quantities were small (<5%). For example, the average C−O distance during adsorption of $CO_{(a)}$ was found by averaging the distance at each time step during adsorption, excluding steps that were less than 600 fs after adsorption and before desorption. If the lifetime of $CO_{(a)}$ on the surface was not long enough to provide sufficient statistics (<1600 fs), the MD run was not used for calculating the C−O distance. We defined a process as adsorption (desorption) if the carbon from CO was within (greater than) 2.7 Å of the closest gold atom for a minimum of 300 fs.

III. Results

A. Simulations of CO Adsorption on Oxygen-Free Au(111). The adsorption of CO on clean Au(111)-(1×1) is weak and leads to a short surface lifetime. The adsorption of CO was simulated on clean Au(111) at 500 K using a $p(3 \times 3)$ unit cell and an unreconstructed Au(111) surface as the starting point. The clean (1×1)-Au(111) surface is used in contrast to the herringbone reconstructed surface for two reasons: first, the experimentally observed herringbone reconstruction of the clean Au(111) surface is often lifted upon adsorption, and second, the difference in surface energy between the ideal (1×1) surface and the surface with the herringbone reconstruction is actually quite small, ∼0.02 eV per surface Au atom.[71] At 500 K, CO should have a very short lifetime on the surface due to its weak adsorption: experimental[72] and theoretical[73] adsorption energies are ∼0.4 and 0.34 eV, respectively. For example, CO adsorption is not detected experimentally at 300 K on Au(111) until high pressures (>0.5 Torr).[74,75] No measurable adsorption of CO at low pressures on Au(110)[15] is detected above 125 K or above 100 K on the oxygen-covered Au(111) surface.[10] We observe qualitatively similar behavior in our simulations: a CO molecule spends only ∼7% of the total simulation time

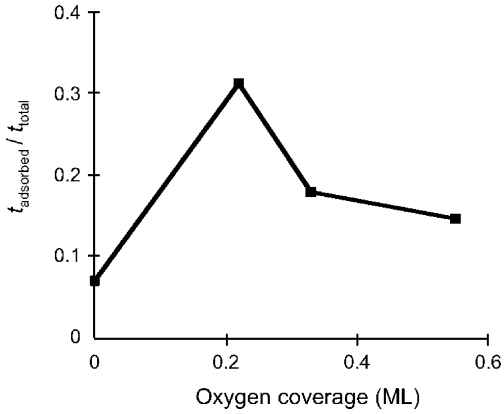

Figure 2. The ratio of time CO spends adsorbed on the surface ($t_{adsorbed}$) to the total simulation time (t_{total}) at different oxygen coverages.

(8 fs) on the surface. Of the 100 independent runs, each of duration 8 fs, CO adsorbs at some point during the simulation for 40% of the runs but quickly desorbs, spending an average of only 861 fs on the surface per adsorption event, resulting in a short overall surface lifetime.

Carbon monoxide preferentially binds to top sites on the (1 × 1)-Au(111) surface, with the carbon interacting with the surface. This is in agreement with experimental[73] and theoretical findings,[76] although one theoretical study finds the 3-fold site to be preferred for CO binding.[26] In our work, we find that the C−O bond is slightly elongated during adsorption, with the gas phase C−O bond of 1.144 Å extending to 1.151 Å during adsorption. These bond distances agree with experimental estimates and static DFT calculations. The experimental gas phase C−O distance[77] is 1.128 Å, while the DFT calculated distance is 1.142 Å in the gas phase and 1.149 Å during adsorption.[63] This elongation is attributed to a slight weakening of the C−O bond, which can be understood as the transfer of electrons from the σ state of CO to the gold surface and back-transfer of electrons from the metal to the π^* state of CO.[78] The C−O bond will increase in length as the binding of CO to gold becomes stronger due to surface defects.[79]

B. CO Adsorption on Oxygen-Covered Au(111). Preadsorption of O on the Au(111) surface increases the surface lifetime of CO and leads to reactive events. Simulations of CO adsorption and oxidation to CO_2 were performed on oxygen-covered Au(111) at three different O coverages—0.22, 0.33, and 0.55 ML—at 500 K. In all cases, CO spends much more time bound to the oxygen-covered surface compared to clean Au(111). For example, CO spends 31% of the total simulation time on the 0.22 ML oxygen-covered surface (Figure 2), compared to 7% of the total simulation time spent adsorbed on the clean surface.

Although lower coverages of O increase the surface lifetime, an increase in the O coverage decreases the residence time of CO compared to adsorption on lower oxygen coverages, to 18% for an O coverage of 0.55 ML. We find the average time CO spends on the surface per adsorption event increase from 861 fs on the clean surface to 2662 fs on 0.22 ML of oxygen on Au(111). Interestingly, this residence time increases to 2903 fs for 0.33 ML of oxygen but then decreases to 2398 fs for 0.55 ML oxygen.

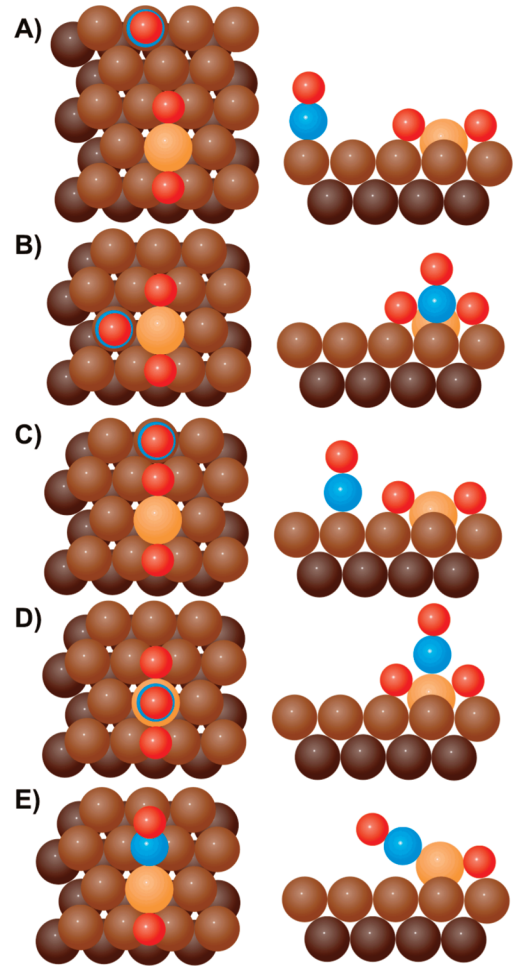

Figure 3. Models of adsorption sites for CO on the oxygen-covered surface, used for the classification of reactions; in the actual simulations, small variations and combinations of these idealized situations are encountered. Brown, gold, blue, and red spheres represent the first layer of gold atoms, a gold adatom lifted out of the first layer of the surface, a carbon atom, and oxygen atom, respectively. In site E, a CO molecule binds on the same gold atom opposite an oxygen atom adsorbed on the surface, causing the gold atom to be lifted from the surface with the CO not bound perpendicular to the surface.

Table 1. Ratio of CO Adsorption Sites at Each Oxygen Coverage[a]

CO site	0.22 ML	0.33 ML	0.55 ML
A	0.63	0.24	0.25
B	0.17	0.11	0.16
C	0.21	0.47	0.00
D	0.00	0.02	0.52
E	0.01	0.16	0.07

[a] The sites are illustrated in Figure 3.

The preferred binding site for CO on the oxygen-covered Au(111) surface is the top site of a gold atom with the CO molecule binding perpendicular to the surface, similar to the clean surface. This configuration clearly predominates for low oxygen coverage (<0.33 ML), since gold adatoms are not as readily formed. Figure 3 and Table 1 illustrate the observed binding sites and distribution of these sites at each coverage.

At higher O coverage, there is a transition in the preferred binding site for CO, partly due to an increase in the number of binding sites around the surface oxide, because this species is more prevalent under these conditions. A transition in CO adsorption sites occurs, changing from sites A and C to site D (Figure 3), as the oxygen coverage increases from 0.33 to 0.55 ML. This corresponds to a change in adsorption from around the AuO_2 surface oxide complex to the site on top of the surface oxide. This is most likely the result of site blocking around the surface oxide complex by oxygen, which leaves only the top of the complex as available binding sites. We also find that CO can pull gold atoms from the surface. Site E (Figure 3) illustrates an adsorption geometry in which a CO molecule binds on a gold atom, which is also bound to an adsorbed oxygen atom. Upon adsorption, this gold atom is lifted from the surface, creating a chain starting with the adsorbed oxygen, a gold adatom, the carbon of the CO, and finally the oxygen from the CO. This configuration has many variations, depending on the type of oxygen surrounding the chain, and it is clear from the wide variation of systems we observed that the coadsorbed system is quite complex and dynamical in nature.

Our calculations also show that there is a strong dependence on the reactivity of oxygen as a function of coverage, in agreement with experiment. Min et al.[16] showed that the reactivity of CO depends on the oxygen coverage: Au(111) oxidized by dosing ozone at 200 K is most reactive at a coverage of ~0.5 ML, with the reactivity decreasing almost linearly with coverage, for either higher or lower oxygen coverage in a classic Langumuir−Hinshelwood behavior. Qualitatively, similar behavior is exhibited in our simulations. For example, reactivity is highest for 0.22 ML oxygen, with about 26% of the independent simulation runs resulting in CO_2 formation. The reactivity decreases to 12% conversion at 0.33 ML and to 8% at 0.55 ML of atomic oxygen coverage.

An ensemble of oxidation reaction pathways exist, with all observed reactions following the Langmuir−Hinshelwood mechanism in which CO adsorption is followed by subsequent reaction, in agreement with the experimental observations of Lazaga et al.[10] Lazaga found a negative activation energy for CO oxidation on Au(111) that was independent of oxygen coverage or CO pressure. The negative activation energy ruled out the possibility of a single elementary reaction step, indicating that CO oxidation does not proceed via an Eley−Rideal mechanism, in which a reaction would occur without CO first adsorbing on the surface. Experimental studies of CO oxidation on Au(111) also are consistent with a Langmuir−Hinshelwood mechanism when O is deposited at low temperature.[16] For clarification, we did occasionally observe CO reaction immediately following adsorption, especially for reaction pathway A_2 in Figure 4, but in all cases CO spends at least a few (>5) vibrational lifetimes on the surface; thus, we define all observed reactions as Langmuir−Hinshelwood. It is important to point out that because of our unphysical initial introduction of CO into the simulation (with zero velocity), we cannot absolutely rule out the possibility of the Eley−Rideal mechanism. However, many adsorption and desorption events occurred during each run, allowing at least the possibility for such a reaction to proceed which we did not observe, in agreement with experimental conclusions.

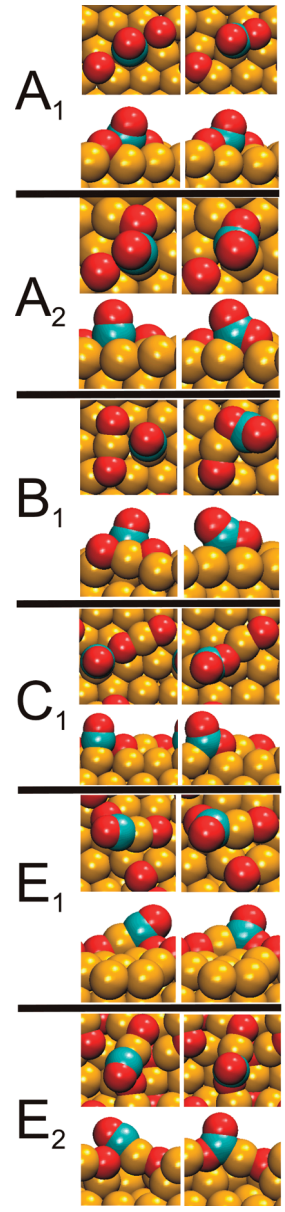

Figure 4. Snapshots (top and side views) of reaction pathways for CO oxidation to CO_2 on oxygen-covered Au(111) surfaces. Yellow, blue, and red spheres represent gold, carbon, and oxygen atoms, respectively. The first column represents the "start" of the reaction, while the second column is approximately the transition state. These defined reaction pathways are used in Table 2. Reactions E_1 and E_2 differ in that CO reacts with a chemisorbed oxygen in the former, while CO reacts with a surface oxide in the latter.

Reactions that involve chemisorbed oxygen atoms proceed primarily through the pathway labeled A_1 in Figure 4. In this pathway, a CO molecule is bound on top of a gold atom neighboring a 3-fold site. During reaction, the CO molecule migrates to the bridge site and toward the oxygen. At the same time, the O atom moves toward the CO through the same 2-fold site. The C of the CO molecule meets the adsorbed oxygen atom, forming CO_2, which then desorbs from the surface since the interaction of CO_2 with the surface

Table 2. Fractional Contribution of Reaction Pathways as a Function of Oxygen Coverage

reaction[a]	0.22 ML	0.33 ML	0.55 ML
A_1	0.77	0.42	0.00
A_2	0.08	0.08	0.50
B_1	0.04	0.00	0.00
C_1	0.12	0.17	0.00
E_1	0.00	0.33	0.00
E_2	0.00	0.00	0.50

[a] The capital letter of each reaction signifies the starting adsorption site (Figure 3) and the subscript refers to each different reaction. Examples of each reaction are illustrated in Figure 4.

is extremely weak.[10] A second, less frequent pathway (see Table 2) for CO reaction with chemisorbed oxygen, labeled A_2 in Figure 4, occurs when CO binds to a gold atom to which oxygen is also bound in a neighboring 3-fold site. The reaction following adsorption is fast due to the instability of the system and because the CO molecule can easily find the adsorbed oxygen atom. Oxidation pathways involving an adsorbed surface oxide complex are initiated in the easiest way from adsorption site C (see Figure 3). A reaction occurs when the CO molecule diffuses toward the adsorbed oxygen. Other reactions involve adsorption site E and occur when the carbon reacts with chemisorbed oxygen (E_1) or the surface oxide or subsurface oxide (E_2). Table 2 lists the ratio of each reaction pathway by coverage. At lower oxygen coverage, reaction pathways involving chemisorbed oxygen (A_1 and A_2 in Figure 4) are dominant; at 0.22 ML of oxygen, chemisorbed oxygen accounts for 88% of the observed reactions. At higher coverages (0.33 and 0.55 ML), reactions with the subsurface oxide and other complicated pathways occur as is commented on in more detail in the Discussion.

IV. Discussion

Using AIMD, we identify two main factors that control the reactivity of CO on oxygen-covered Au(111): (1) the ability of CO to adsorb on the surface and (2) the local binding of the adsorbed oxygen. Our simulations are in general agreement with experiment and prior static DFT calculations. We find that the structure of the oxygen-covered surface and the oxygen coverage affect the CO oxidation pathways that contribute. CO oxidation was studied in a number of static DFT calculations; Su et al.[25] found a barrier of 0.29 eV for the oxidation on the Au(111) surface, while Liu et al.[26] found a barrier of 0.25 eV for the same reaction on the Au(221) surface. The careful recent DFT work of Wang et al. also showed how the barrier and rate for CO oxidation could strongly depend on surface structure and coordination of gold atoms.[80] We find similar trends, but importantly, we find the most reactive surface to be the one with 0.22 ML of oxygen, which contains oxygen mostly bound in 3-fold sites.

We attribute the increased binding of CO to the oxygen-covered surface to the presence of under-coordinated gold atoms that form upon adsorption of oxygen. Earlier theoretical[64] and experimental[81] work has shown that the gold surface becomes rough upon adsorption of oxygen, leading to a higher concentration of under-coordinated surface gold atoms as the O concentration increases. Under-coordinated Au atoms have been proposed to enhance the activity for O_2 dissociation for a variety of systems, including supported Au nanoparticles[32,39,76,82,83] and Au clusters on Au(111).[46,80]

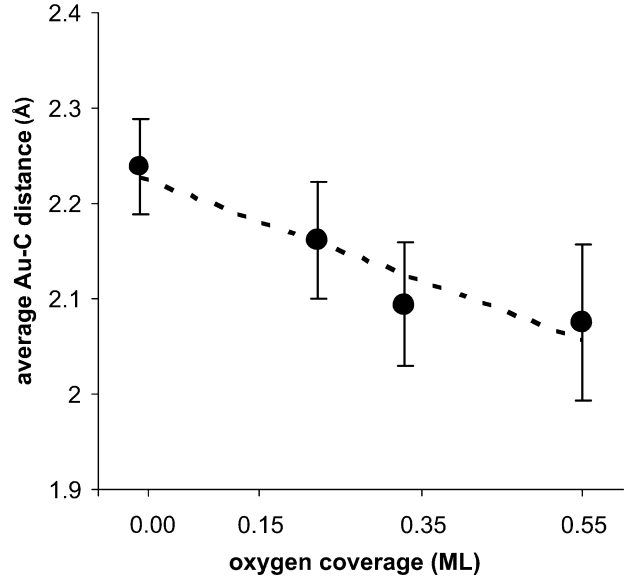

Figure 5. Average $Au-C_{(CO)}$ distance for adsorbed CO as a function of oxygen coverage.

The increasing roughness of the surface with oxygen coverage is expected to increase the binding strength of CO, based on studies by Wang et al.,[80] who found that the CO adsorption strength was inversely proportional to the coordination of the gold atom to which the CO is bound. In fact, by analyzing the average bond length of the carbon atom within CO to the gold atom on the surface to which it is bound, we observe a slight, but systematic, decrease in the bond length with increasing oxygen coverage (Figure 5), suggesting that CO adsorption is stronger on the rougher surface, which contains a larger number of under-coordinated gold. However, at O coverages greater than 0.22 ML, we observe a decrease in the CO surface lifetime, in agreement with previous experimental observations.[17] This suggests that while the binding of CO to the surface is stronger at higher oxygen coverage, the additional adsorbed oxygen is blocking sites for adsorption.

Since the reaction follows the Langmuir−Hinshelwood mechanism, adsorption of CO is an important first step to reaction. We find a strong correlation between the CO surface lifetime and the rate of oxidation. Despite the stronger CO adsorption at higher oxygen coverage, due to site blocking, the CO spends less time adsorbed on the surface. Since CO spends less time on the surface, there is less probability to react, leading to a lower oxidation rate.

It is important to understand the role of the type of oxygen involved in the reaction, that is, whether oxygen is chemisorbed or takes the form of a surface or subsurface oxide. The probability of CO adsorption alone cannot explain the reactivity trends, since the reaction rate decreases as a function of coverage, even when the reaction probability is normalized by the fraction of time CO spends adsorbed on the surface. We also expect that the reaction energy barriers and the availability to attack should significantly differ, depending on the oxygen species.

Table 3. Ratio of Chemisorbed Oxygen and Surface Oxide on the Surface before CO Oxidation (Surface Species) and the Oxygen Atom Type Consumed during Oxidation (Reactive Species) along with the Relative Rate and Normalized Relative Rate (By Oxygen Type) for the Reaction for Each Oxygen Type on 0.22 and 0.33 ML Oxygen Covered Au(111)

	0.22 ML		0.33 ML	
	chemisorbed	surface oxide	chemisorbed	surface oxide
surface species	0.80	0.20	0.60	0.40
reactive species	0.88	0.12	0.83	0.17
relative rate	7.7	1.0	5.0	1.0
normalized relative rate	1.9	1.0	3.3	1.0

We find chemisorbed oxygen to be the most reactive oxygen species for CO oxidation. This effect is illustrated in Table 3, which compares the amounts of each oxygen type present at 0.22 and 0.33 ML relative to the probability that they react with CO to form CO_2. At both oxygen coverages, the chemisorbed oxygen contributes to the majority of the oxidation reactions. For 0.22 ML of oxygen coverage, initially 80% of the surface is covered with chemisorbed oxygen while 20% is covered with surface oxide. However, of the oxygen types responsible for oxidation, 88% is chemisorbed oxygen. The same is true for 0.33 ML of oxygen coverage: the surface is covered with 60% of chemisorbed oxygen, yet chemisorbed oxygen makes up 83% of the reactive atoms, illustrating that the chemisorbed oxygen is the most reactive type on the surface. Table 3 also illustrates the calculated relative reaction rate for each oxygen type. Even when the rate is normalized to take into account the ratio of each oxygen species on the surface (bottom line of Table 3), the relative rate for reaction with chemisorbed oxygen is significantly higher than surface oxide.

V. Conclusions

Realistic simulation of catalytic reactions on surfaces is an important endeavor that requires substantial computational resources. Generally, two key factors need to be taken into consideration when simulating such systems: the ability to accurately describe the important characteristics of the system (such as the forces between nuclei, charge transfer, etc.) and the need to minimize the computational cost of the simulation so that the dynamics of the system can be modeled for long time scales. Coarse-grained and lattice-based methods, such as kMC, are capable of investigating processes over a long time scale, but these methods must simplify the complicated electronic and ionic system using approximations or reduce the dimensionality of the fully atomistic system to a lattice. For systems as complicated as the interaction of oxygen on gold, neither of these approximations is acceptable, because oversimplifying the system features makes the simulation unreliable. To avoid this problem, we have used a fully atomistic simulation with forces between nuclei accurately calculated using DFT. This level of accuracy is computationally costly, resulting in dynamical runs that extend only for ~10 ps and small unit cells, which may artificially restrict the possible structures that could be observed computationally. Furthermore, we cannot model the effect of the initial CO velocity on the reaction, since we introduced CO into the system with a zero velocity because of computational cost. Nevertheless, a number of useful conclusions can be obtained from these simulations.

The oxidation of CO on Au(111) is a prototypical model system for ab initio molecular dynamics simulations, due to its inherent interest, involving a representative simple molecule that can be oxidized and an originally inert solid surface on which atomic-scale features can play an important role in reactivity. We carried out an extensive study of this system, using AIMD simulations. We find the highest rate of CO oxidation for 0.22 ML of oxygen coverage, with decreasing activity at the other two oxygen-coverage conditions we considered, 0.33 and 0.55 ML. The difference in reactivity that we found is most likely due to two factors: the type of oxygen atoms present on the surface during reaction and the ability of CO to adsorb on the surface. We have identified chemisorbed oxygen as the most reactive type of oxygen atoms. Furthermore, we observe a decrease in the adsorption probability for CO with increasing oxygen coverage, despite the increase in the strength of CO adsorption. The decrease in the probability for CO adsorption results in a decrease in reactivity as the oxygen coverage increases.

Acknowledgment. This work was funded in part by a NSF grant via Harvard NSEC, grant no.PHYS-0646094. We thank the Cyber-Infrastructure Laboratory of the Harvard School of Engineering and Applied Sciences and the Faculty of Arts and Sciences Research Computing group for computational resources. We acknowledge useful discussions with Xiaoying Liu and Bingjun Xu.

References

(1) Haruta, M. *Chem. Rec.* **2003**, *3*, 75.

(2) Haruta, M.; Date, M. *Appl. Catal. A-Gen.* **2001**, *222*, 427.

(3) Meyer, R.; Lemire, C.; Shaikhutdinov, S. K.; Freund, H. *Gold Bull.* **2004**, *37*, 72.

(4) Haruta, M.; Yamada, N.; Kobayashi, T.; Iijima, S. *J. Catal.* **1989**, *115*, 301.

(5) Hayashi, T.; Tanaka, K.; Haruta, M. *J. Catal.* **1998**, *178*, 566.

(6) Grisel, R. J. H.; Kooyman, P. J.; Nieuwenhuys, B. E. *J. Catal.* **2000**, *191*, 430.

(7) Jang, B. W. L.; Spivey, J. J.; Kung, M. C.; Kung, H. H. *Energy Fuels* **1997**, *11*, 299.

(8) Thompson, D. *Gold Bull.* **2000**, *33*, 40.

(9) Haruta, M.; Kobayashi, T.; Sano, H.; Yamada, N. *Chem. Lett.* **1987**, 405.

(10) Lazaga, M. A.; Wickham, D. T.; Parker, D. H.; Kastanas, G. N.; Koel, B. E. *ACS Symp. Ser.* **1993**, *523*, 90.

(11) Min, B. K.; Friend, C. M. *Chem. Rev.* **2007**, *107*, 2709.

(12) Kim, J.; Samano, E.; Koel, B. E. *J. Phys. Chem. B* **2006**, *110*, 17512.

(13) Stiehl, J. D.; Kim, T. S.; McClure, S. M.; Mullins, C. B. *J. Am. Chem. Soc.* **2004**, *126*, 13574.

(14) Gottfried, J. M.; Christmann, K. *Surf. Sci.* **2004**, *566*, 1112.

(15) Outka, D. A.; Madix, R. J. *Surf. Sci.* **1987**, *179*, 351.

(16) Min, B. K.; Alemozafar, A. R.; Pinnaduwage, D.; Deng, X.; Friend, C. M. *J. Phys. Chem. B* **2006**, *110*, 19833.

(17) Ojifinni, R. A.; Froemming, N. S.; Gong, J.; Pan, M.; Kim, T. S.; White, J. M.; Henkelman, G.; Mullins, C. B. *J. Am. Chem. Soc.* **2008**, *130*, 6801.

(18) Kim, T. S.; Gong, J.; Ojifinni, R. A.; White, J. M.; Mullins, C. B. *J. Am. Chem. Soc.* **2006**, *128*, 6282.

(19) Gottfried, J. M.; Christmann, K. *Surf. Sci.* **2004**, *566*, 1112.

(20) Yoon, B.; Hakkinen, H.; Landman, U.; Worz, A. S.; Antonietti, J. M.; Abbet, S.; Judai, K.; Heiz, U. *Science* **2005**, *307*, 403.

(21) Broqvist, P.; Molina, L. M.; Gronbeck, H.; Hammer, B. *J. Catal.* **2004**, *227*, 217.

(22) Molina, L. M.; Rasmussen, M. D.; Hammer, B. *J. Chem. Phys.* **2004**, *120*, 7673.

(23) Molina, L. M.; Hammer, B. *Phys. Rev. B* **2004**, *69*, 155424.

(24) Coquet, R.; Howard, K. L.; Willock, D. J. *Chem. Soc. Rev.* **2008**, *37*, 2046.

(25) Su, H. Y.; Yang, M. M.; Bao, X. H.; Li, W. X. *J. Phys. Chem. C* **2008**, *112*, 17303.

(26) Liu, Z. P.; Hu, P.; Alavi, A. *J. Am. Chem. Soc.* **2002**, *124*, 14770.

(27) Prestianni, A.; Martorana, A.; Ciofini, I.; Labat, F.; Adamo, C. *J. Phys. Chem. C* **2008**, *112*, 18061.

(28) Fajin, J. L. C.; Cordeiro, M.; Gomes, J. R. B. *J. Phys. Chem. C* **2008**, *112*, 17291.

(29) Chen, Y.; Crawford, P.; Hu, P. *Catal. Lett.* **2007**, *119*, 21.

(30) Wang, C. M.; Fan, K. N.; Liu, Z. P. *J. Am. Chem. Soc.* **2007**, *129*, 2642.

(31) Ganesh, R.; Pala, S.; Liu, F. *J. Chem. Phys.* **2006**, *125*, 5.

(32) Lopez, N.; Janssens, T. V. W.; Clausen, B. S.; Xu, Y.; Mavrikakis, M.; Bligaard, T.; Norskov, J. K. *J. Catal.* **2004**, *223*, 232.

(33) Zhang, C. J.; Hu, P. *J. Am. Chem. Soc.* **2000**, *122*, 2134.

(34) Molina, L. M.; Lesarri, A.; Alonso, J. A. *Chem. Phys. Lett.* **2009**, *468*, 201.

(35) Liu, L. M.; McAllister, B.; Ye, H. Q.; Hu, P. *J. Am. Chem. Soc.* **2006**, *128*, 4017.

(36) Liu, Z. P.; Jenkins, S. J.; King, D. A. *Phys. Rev. Lett.* **2004**, *93*, 156102.

(37) Liu, Z. P.; Gong, X. Q.; Kohanoff, J.; Sanchez, C.; Hu, P. *Phys. Rev. Lett.* **2003**, *91*, 266102.

(38) Kandoi, S.; Gokhale, A. A.; Grabow, L. C.; Dumesic, J. A.; Mavrikakis, M. *Catal. Lett.* **2003**, *93*, 93.

(39) Remediakis, I. N.; Lopez, N.; Norskov, J. K. *Angew. Chem., Int. Ed.* **2005**, *44*, 1824.

(40) Baker, T. A.; Xu, B.; Friend, C. M.; Kaxiras, E. Unpublished, 2009.

(41) Valden, M.; Lai, X.; Goodman, D. W. *Science* **1998**, *281*, 1647.

(42) Valden, M.; Pak, S.; Lai, X.; Goodman, D. W. *Catal. Lett.* **1998**, *56*, 7.

(43) Comotti, M.; Li, W. C.; Spliethoff, B.; Schuth, F. *J. Am. Chem. Soc.* **2006**, *128*, 917.

(44) Xu, Y.; Mavrikakis, M. *J. Phys. Chem. B* **2003**, *107*, 9298.

(45) Yoon, B.; Hakkinen, H.; Landman, U. *J. Phys. Chem. A.* **2003**, *107*, 4066.

(46) Mills, G.; Gordon, M. S.; Metiu, H. *J. Chem. Phys.* **2003**, *118*, 4198.

(47) Stiehl, J. D.; Kim, T. S.; McClure, S. M.; Mullins, C. B. *J. Am. Chem. Soc.* **2004**, *126*, 1606.

(48) Deng, X. Y.; Min, B. K.; Guloy, A.; Friend, C. M. *J. Am. Chem. Soc.* **2005**, *127*, 9267.

(49) Wang, J.; Voss, M. R.; Busse, H.; Koel, B. E. *J. Phys. Chem. B* **1998**, *102*, 4693.

(50) Gottfried, J. M.; Elghobashi, N.; Schroeder, S. L. M.; Christmann, K. *Surf. Sci.* **2003**, *523*, 89.

(51) Biener, M. M.; Biener, J.; Friend, C. M. *Surf. Sci.* **2005**, *590*, L259.

(52) Canning, N. D. S.; Outka, D.; Madix, R. J. *Surf. Sci.* **1984**, *141*, 240.

(53) Saliba, N.; Parker, D. H.; Koel, B. E. *Surf. Sci.* **1998**, *410*, 270.

(54) Battaile, C. C.; Srolovitz, D. J. *Annu. Rev. Mater. Res.* **2002**, *32*, 297.

(55) Reuter, K.; Scheffler, M. *Phys. Rev. B* **2006**, *73*, 045433.

(56) Rapaport, D. C. *The Art of Molecular Dynamics Simulation*; Cambridge University Press: Cambridge, 2004; pp 1−10.

(57) Radeke, M. R.; Carter, E. A. *Annu. Rev. Phys. Chem.* **1997**, *48*, 243.

(58) Marx, D.; Hutter, J. *Ab Initio Molecular Dynamics: Basic Theory and Advanced Methods*; Cambridge University Press: Cambridge, 2009; pp 369−406.

(59) Wodtke, A. M.; Tully, J. C.; Auerbach, D. J. *Int. Rev. Phys. Chem.* **2004**, *23*, 513.

(60) Tully, J. C. *Annu. Rev. Phys. Chem.* **2000**, *51*, 153.

(61) Car, R.; Parrinello, M. *Phys. Rev. Lett.* **1985**, *55*, 2471.

(62) Tully, J. C. In *Modern Methods for Multidimensional Dynamics Computations in Chemistry*; Thompson, D. L., Ed.; World Scientific: Singapore, 1998; pp 34−72.

(63) Tully, J. C. In *Classical and Quantum Dynamics in Condensed Phase Simulations*; Berne, B. J., Ciccotti, G., Coker, D. F., Eds.; World Scientific: Singapore, 1998; pp489−514.

(64) Baker, T. A.; Xu, B.; Liu, X.; Friend, C. M.; Kaxiras, E. *J. Phys. Chem.* **2009**, *113*, 16561.

(65) Nose, S. *Mol. Phys.* **2002**, *100*, 191.

(66) Kresse, G.; Hafner, J. *Phys. Rev. B* **1993**, *47*, 558.

(67) Vanderbilt, D. *Phys. Rev. B* **1990**, *41*, 7892.

(68) Kresse, G.; Hafner, J. *J. Phys.-Condes. Matter* **1994**, *6*, 8245.

(69) Perdew, J. P.; Wang, Y. *Phys. Rev. B* **1992**, *45*, 13244.

(70) King, D. A.; Wells, M. G. *Surf. Sci.* **1972**, *29*, 454.

(71) Wang, Y.; Hush, N. S.; Reimers, J. R. *Phys. Rev. B* **2007**, *75*, 233416.

(72) Elliott, G. S. Thesis, University of California, San Diego, 1988.

(73) Piccolo, L.; Loffreda, D.; Ladete Santos Aires, F. J.; Deranlot, C.; Jugnet, Y.; Sautet, P.; Bertolini, J. C. *Surf. Sci.* **2004**, *566−568*, 995.

(74) Nakamura, I.; Takahaski, A.; Fujitani, T. *Catal. Lett.* **2009**, *129*, 400.

(75) Peters, K. F.; Steadman, P.; Isern, H.; Alvarez, J.; Ferrer, S. *Surf. Sci.* **2000**, *467*, 10.

(76) Mavrikakis, M.; Stoltze, P.; Morskov, J. K. *Catal. Lett.* **2000**, *64*, 101.

(77) *CRC Handbook of Chemistry and Physics*, 77th ed.; Lide, D. R., Ed.; CRC Press: New York, 1996; pp 9−17.

(78) Shriver, D.; Atkins, P. *Inorganic Chemistry*; W. H. Freeman and Co.: New York, 2003; pp 544−546.

(79) Loffreda, D.; Sautet, P. *J. Phys. Chem. B* **2005**, *109*, 9596.

(80) Wang, H. F.; Gong, X. Q.; Guo, Y. L.; Guo, Y., G. L.; Hu, P. *J. Phys. Chem. C* **2009**, *113*, 6124.

(81) Min, B. K.; Deng, X.; Pinnaduwage, D.; Schalek, R.; Friend, C. M. *Phys. Rev. B* **2005**, *72*, 4.

(82) Lopez, N.; Norskov, J. K. *J. Am. Chem. Soc.* **2002**, *124*, 11262.

(83) Lemire, C.; Meyer, R.; Shaikhutdinov, S.; Freund, H. J. *Angew. Chem., Int. Ed.* **2004**, *43*, 118.

CT9004596